Artificial Neural Network and ESPRIT-TLS Combination-Based Approach for Fault Bearing Recognition in Induction Machines

Pascal Dore[1†], **Saad Chakkor**[1], **Mostafa Baghouri**[2], and **Ahmed El Oualkadi**[1], Non-members

ABSTRACT

Several studies have been conducted in recent decades on the detection of bearing faults to develop methods for real-time monitoring. Faults are found in almost all electromechanical systems and the major cause of damage to machinery, resulting in serious accidents to humans and material environments. While methods such as MCSA (Motor Current Signature Analysis) and PCA (Principal Component Analysis) have been widely used for obtaining and analyzing the machine's stator current and reducing its dimensions and noise, they do not allow for easier detection and parameter estimation when a defect appears, and sometimes help from an expert is needed to explain the signals. In this paper, the use of ANN-GA (Artificial Neural Networks-Genetic Algorithm) is investigated in combination with the best variant of the ESPRIT (Estimation of Signal Parameters via Rotational Invariant Techniques) method applied on stator current signals for efficient real-time bearing fault detection, to avoid any help being required from experts. MATLAB simulations of these variants revealed that the TLS variant highly discriminates the fault. By using this variant to prepare the data in the search of the best ANN model, in combination with genetic algorithms (used for optimizing the search of ANN parameters), two architectures capable of discriminating this bearing fault in real time in time and frequency domain were obtained.

Keywords: Bearing Fault, Automatic Monitoring, Classification, Genetic Algorithm, Artificial Neural Networks, ESPRIT

1. INTRODUCTION

In this study, the combination and application of MCSA are used with classical high-resolution signal processing (HRM) methods and artificial intelligence algorithms to diagnose electromechanical faults in electrical induction machines. In the past, combinations of MCSA, PCA, and other signal processing methods have also been used to accomplish the same task. These methods include FFT [1] (Fast Fourier Transform), STFT (Short Time Fourier Transform), and PCA [2, 3]. However, although these algorithms have been able to address this issue in their own way, it should be noted that bearing fault detection, the most common in electrical induction machines, has always given rise to a variety of topics, [4–15] to solve the problem of monitoring these bearings. It should be noted that they all have limitations. Furthermore, MCSA, which is based on spectral analysis, has been widely used in the detection and diagnosis of faults in electric induction machines. It has delivered satisfactory results in a wide range of industrial applications. However, because of the following practical limitations, this technique can lead to incorrect diagnostic conclusions:

- The variation in load conditions during the sampling period; the harmonics of a slip dependent fault vary with speed. As a result, fault identification becomes more difficult, and diagnostic accuracy suffers.
- Mechanical vibration frequencies are mixed up. The reduction in speed of certain devices, such as the gearbox, or the effect of the oscillating load, can generate similar side frequencies to those caused by actual faults.

All these disadvantages have necessitated the development and integration of new diagnostic methods based on advanced artificial intelligence tools. This has prompted researchers to gradually migrate to more appropriate solutions, leading to the selection of this association, which, in addition to being independent of the system under study, provides an intelligent, accurate, and adaptable diagnosis as the machine operates.

Thus, the desire is to develop systems or procedures to detect these failures from the start, particularly at their inception. Several methods, including the ANN, have been evidenced. The only problem with this approach is that the parameterization of the final model can be greedy in terms of the number of layers used and the time required to train this artificial neural network. The genetic algorithm is used to improve this task. It enables the rapid development of highly effective solutions to this problem. The main advantage of this algorithm is that it does not require starting examples to learn, or a basis to

Manuscript received on February 14, 2022; revised on May 23, 2022; accepted on July 20, 2022. This paper was recommended by Associate Editor Piya Kovintavewat.

[1]The authors are with the Laborattory of Information and Communication Technologies (LabTIC), National School of Applied Sciences of Tangier (ENSATg), University of Abdelmalek Essaâdi, Tangier, Morocco.

[2]The author is with the Laboratory LCCPS, ENSAM de Casablanca, Hassan II University, Casablanca, Morocco.

[†]Corresponding author: dore.pascal@etu.uae.ac.ma

Digital Object Identifier: 10.37936/ecti-eec.2023211.248598

learn.

As a result, using vibratory, ultrasonic, or thermal methods to acquire signals from the monitored machine, which uses contact sensors or, in some cases, human presence, is no longer necessary. The noise generated by these sensors in the event of a bad fixation must be considered since this can result in several false positives. The MCSA (Machine Current Signature Analysis) method is used in this study.

2. PROBLEM FORMULATION

The rolling defect, MCSA method, and the ESPRIT algorithm are discussed in this study and along with the reasons for choosing these two techniques over others.

The artificial neural networks and their relationship with genetic algorithms are then discussed. Before concluding with the perspectives, the results obtained are presented and the ANN-GA association on the training data prepared with the ESPRIT-TLS in the fourth section.

2.1 Bearing Fault Modeling and Detection

According to the literature, the most common causes of failure in rotating machines are spalling, fatigue, lubricant contamination or deficiency, excessive load, or electrical causes such as inverter-induced current flow leakage [16]. Bearing faults cause a variety of effects in rotating machines, ranging from increased vibration and noise level variations (oscillations) in the machine load torque (resulting in rotor stall) to eccentricity faults, which are a major cause of internal magnetic flux variation and produce harmonics in the stator current [17, 18]. Fig. 1 depicts a bearing and the faults it can cause, namely inner ring damage, outer ring damage, and cage fault. The bearing fault is denoted by the following formula:

$$f_{bng} = \left| f_0 \pm k f_{i,o} \right| \tag{1}$$

where $k = 1, \ldots, N$, and

$$f_{i,o} = \begin{cases} 0.4 f_r \\ 0.6 f_r \end{cases} \tag{2}$$

where f_r is the rotor frequency, $f_{i,o}$ is any inner or outer frequency; it depends on the dimensions and characteristics of vibration of the bearings, f_0 is the power supply frequency, and k represents an integer which conditions the harmonics of the fault in the stator signal.

2.2 MCSA Approach

Some earlier methods like measurement by vibration, ultrason, and thermal were used to obtain the signal from the induction machines, although in the last decade MCSA has been largely used. This is because it provides an easy way to obtain the stator current from these machines by avoiding any physical contact with them,

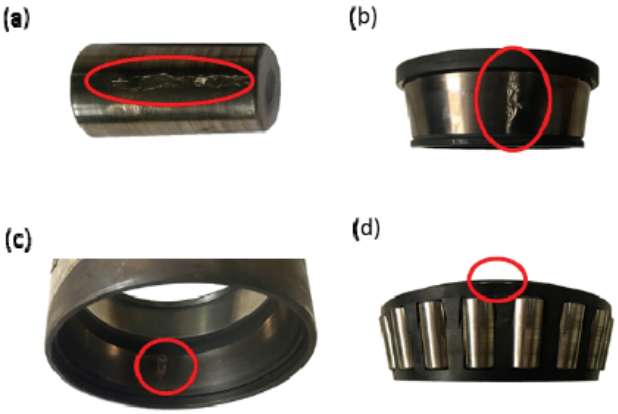

Fig. 1: (a) Ball fault, (b) inner ring damage, (c) outer ring damage, and (d) cage fault.

while other techniques do not. Motor current signature analysis (MCSA) is a rotating machine condition monitoring technique used to diagnose problems in induction machines [19, 20]. The concept originated in the early 1970s and was first proposed for use in nuclear power plants for inaccessible motors located in hostile or hazardous areas [21]. However, over time, it quickly gained popularity in the industry, especially for the monitoring of rotating machinery.

2.2.1 Modeling of the stator current in the asynchronous machine

The use of the stator current for monitoring rotating machines is useful for three main reasons: as a first step, it can be used to diagnose electrical and mechanical faults such as phase imbalance, short circuit in stator windings, bearing failure, bent shaft, broken bar, etc. Secondly, the stator current is very easy to access because it is directly measurable and used to control the machine itself, and thirdly, it can be modeled mathematically. Therefore, if we know the characteristics of the fault, it is easy to model the stator current of the machine operating in generator mode without forgetting. However, this analytical model of the signal must accurately describe the behavior and evolution of the real stator current.

To study the detection of the previously mentioned faults, the stator current of the asynchronous machine is designated by the discrete signal x. This is obtained by sampling the direct current $x(t)$ with a step equal to $T_s = 1/F_s$. This discrete stator current $x[n]$ of the electric induction machine in the presence of mechanical and/or electrical failures is expressed as follows [22]:

$$x[n] = \sum_{k=-L}^{L} a_k \cos\left(2\pi f_k (w(n)) \times \frac{n}{F_k} + \Phi_k\right) + b[n] \tag{3}$$

where $x[n]$ corresponds to a single sample of the stator current. $b[n]$ is a sample of Gaussian noise. The

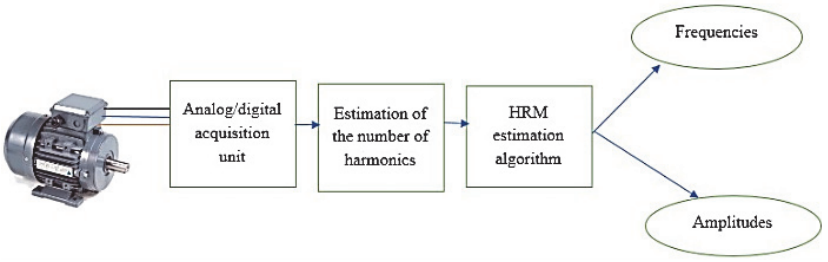

Fig. 2: *Fault detection procedure with an HRM.*

parameter L is the number of side frequencies introduced by malfunctions. The quantities $f_k(w(n))$, a_k, and Φ_k correspond to frequency, amplitude, and phase respectively. $w(n)$ is a parameter to be estimated at each instant of order n, depending on the studied fault.

The representation of this signal in the time domain is not sufficient to properly diagnose the states of the machine at a given instant. It is for this reason that the four methods presented earlier are combined for the total exploitation of all the information contained in this composite signal.

2.3 ESPRIT Method and Its Variants

Among all the signal processing techniques used to analyze the stator signal, ESPRIT has gained major applicability compared to other techniques [1]. This is because it allows the best estimation, with flexibility and the ability to understand the signal composition. In contrast to EMD, VMD, or HHT, it does not require pre-treatment of the signal to do its work.

ESPRIT is an estimating method for signal parameters using the rotational invariance technique. This algorithm detects the spectral components (harmonics) contained in a signal with very high accuracy in frequency and amplitude estimation, independent of the observation window size used. It is an appropriate approach for obtaining reliable spectral estimation results without synchronization effects [22, 23]. It is based on shift invariance. It exists naturally between the discrete-time series leading to rotational invariance and the corresponding signal subspaces.

In this case, the eigenvectors U of the signal autocorrelation matrix define two subspaces (signal and noise) using two selection matrices γ_1 and γ_2.

$$S_1 = \gamma_1 U, \quad S_2 = \gamma_2 U \tag{4}$$

The rotational invariance between the two subspaces leads to the following equation:

$$S_1 = \Phi S_2 \tag{5}$$

where

$$\Phi = \begin{bmatrix} e^{j2\pi f_1} & 0 & \cdots & 0 \\ 0 & e^{j2\pi f_2} & \cdots & 0 \\ \vdots & \vdots & \cdots & \vdots \\ 0 & 0 & \cdots & e^{j2\pi f_N} \end{bmatrix} \tag{6}$$

The matrix Φ contains all the information on the N frequency components. The estimated matrices S_1 and S_2 may contain errors [10]. The determination of this matrix allows the estimates of the frequency to be obtained, as defined by the following formula:

$$f_k = \frac{Arg\left(\Phi_{k,k}\right)}{2\pi} \tag{7}$$

where $k = 1, 2, \ldots, N$.

The application of all these methods makes it possible to carry out a comparison between their performances. They are used in the detection of faults that may occur in an electric induction machine.

In this study, six variants of the ESPRIT algorithm along with their roots are used to estimate the frequencies and amplitudes contained in the stator current signal of the machine. Other than the ESPRIT-TLS variant which takes as its argument a third parameter, namely the window length, these variants take two essential parameters: the signal vector and the harmonics number or the estimation mode based on the model order selection (MOS). These variants are: ESPRIT-TLS, ESPRIT-ITCMP, ESPRIT-SVDSSA, ESPRIT-IRLBA, ESPRIT-SVD, ESPRIT-ECON. The procedure for estimating the frequencies and amplitudes of faults by these variants is given in Fig. 2.

In terms of TLS, ESPRIT-TLS is a variant of the ESPRIT method, employing TLS to estimate the parameters of a composite signal. In other words, with this property, it can extract the various frequencies and amplitudes contained in the signal. The Total Least Squares (TLS) method is an error compensation technique. It was first used to solve TLS problems [13] through singular value decomposition (SVD). TLS can be solved using both direct and iterative methods. The SVD is computed directly using direct methods. It accepts three parameters as input:

X: the signal vector.

p: the number of characteristic harmonics of the

signal. It is determined by the MOS.

$$p = \text{round}\left(\frac{2 \times N}{3}\right) \tag{8}$$

where N is the number of samples.
M: length of the observation window.

It works as follows:

- calculation of the augmented data matrix,
- calculation of the SVD of the augmented matrix,
- set up the signal subspace,
- split this subspace into two subspaces,
- calculate the rotation between these two subspaces,
- calculate the rotation for the original data,
- estimate the frequencies,
- calculate the complex amplitudes,
- estimate the amplitudes,
- return the estimated frequencies and amplitudes.

3. ARTIFICIAL NEURAL NETWORKS AND GENETIC ALGORITHM

3.1 Artificial Neural Networks

Even though humans can be useful in some situations, they may not be in others because they are tired, sleeping, or eating. This is true, for example, of tasks requiring greater concentration and dexterity. A single moment of distraction can destroy an entire arsenal. This is where ANNs come into play since their only failure mode is a power outage. These algorithms, when properly trained, are capable of great feats and tasks such as surveillance, decision-making, and others. For this reason, they are used to automate the monitoring system for induction machines, which can suffer damage at any time.

Artificial neural networks based on the functioning of the human brain are developed in the form of parallel distributed network models [24]. These networks are composed of input layers, hidden layers, and output layers. In each layer, numbers of variable neurons are conditioned by weight, bias, and an activation function, and it should be noted that the number of neurons at the level of the hidden layers play an important role in the final nature of the model thus formed. With this configuration, like the human brain, they learn to solve problems like detection and classification by avoiding any intervention from experts. Today, there are several types of networks depending on the need. This study is interested in the multi-layer perceptions. Fig. 3 shows an example of ANN.

The principle is that they take data as input and build an image or trace the analyzed data by successively passing it through the levels of layers, which condition the output.

Considering the input vectors

$$X = \left[x_1, x_2, \cdots, x_n\right]^T \tag{9}$$

where x_i are the rows or columns of features used to train or research the architecture of ANN needed, by using the

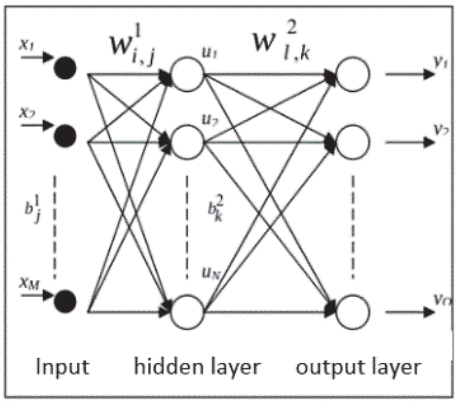

Fig. 3: *Example of a multi-layer perceptron.*

activation function f_j, the input vectors are transformed to an intermediate vector of the hidden variables U.

The hidden layer j-th neurons' output U_j is obtained as follows:

$$U_j = f_{jH}\left(\sum_{i=1}^{M} W_{i,j}^{H} \times x_i \; + \; b_j^H\right) \tag{10}$$

where b_j^H and $W_{i,j}^H$ represent the bias and weight between the j-th neuron of the hidden layer (or next hidden layer) and the i-th neuron of the input layer, respectively (or next hidden layer). The hidden connection between the neurons of the input (or intermediate layer)/hidden layers is represented by the upper index H.

The output vectors that are desired

$$Y = \left[y_n, y_{n-1}, \cdots, y_0\right]^T \tag{11}$$

of the network are obtained from the vector of intermediate variables U_{lH} by an activation function fout of the output layer. For example, the output of the neuron is expressed as follows:

$$y_k = f_{out}\left(\sum_{i=l}^{M} W_{l,k}^{H} \times U_{l,k} + b_k^H\right) \tag{12}$$

where the sub-index *out* denotes the (last) connection between the neurons of the hidden/output layers. There are several activation functions, f_{jH} and f_{out}, such as the sigmoid function, the hyperbolic tangent, the linear function, and the softmax function given by Eqs. (13) to (16), respectively:

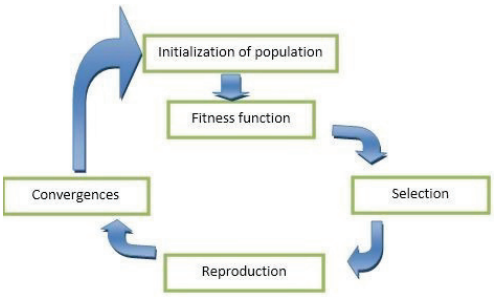

Fig. 4: Principle of the genetic algorithm.

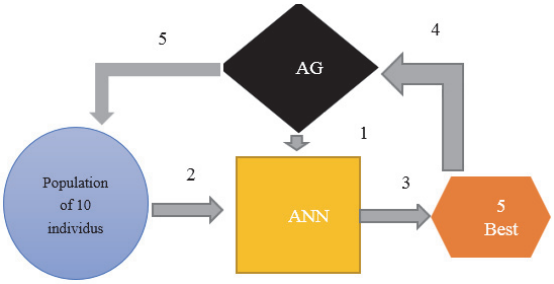

Fig. 5: Association of the ANN and GA. (2) starts with 10 ANN individuals, on which the genetic algorithm in (1) is applied by intervening the data, leaving five architectures capable of identifying the defect in (3). Then, in (4), these five pass in the GA, resulting in a new population in (5). The cycle then repeats itself until the desired generation is reached.

$$f(v) = \frac{1}{1 + e^{-v}} \tag{13}$$

$$f(v) = \frac{1 - e^{-2v}}{1 + e^{-2v}} \tag{14}$$

$$f(v) = v \tag{15}$$

$$f(v) = \frac{e^{v_i}}{\sum_{j=1}^{k} e^{v_j}} \tag{16}$$

3.2 Genetic Algorithms

It is possible to obtain ANN alone by changing its parameter architectures to help to solve a classification problem. However, sometimes, it is very difficult to make a perfect model by tuning the parameters one by one or all at once, and even if this is possible, it would take a long time to give an optimized model. Therefore, another method is required. That is why in the last decades the power optimization algorithm has been used to achieve this, among them the genetic algorithm.

The goal of using a genetic algorithm in this study is to find an optimal architecture giving good precision in the classification of the machine state with faster fault detection or even in real time [25]. The necessary steps to achieve its employability are illustrated in Fig. 4:

- the chromosome code which consists of finding the nature of the genes that will form the individuals of the process;
- the generation of the population which gives it the means to make the first choice of a set of starting individuals;
- the evolution which consists of the creation of new individuals by the operations of mutation and crossing.

Table 1: Simulation parameters.

Parameters	Values
Rotor frequency (f_r)	29.01 Hz
Power supply frequency (f_0)	50 Hz
Indoor/outdoor frequency ($f_{i,o}$), depending on the dimensions and characteristics of the vibration in the bearings	139.248 Hz
Number of balls in a bearing (n_b)	12
Sampling frequency (F_s)	1000 Hz
Conditions the harmonics of the fault in the stator signal (k)	1
Signal to noise ratio (SNR)	[0–102] dB
Amplitude of the stator (a_0)	10 A
Processor	Intel Pentium® CPU B950 @ 2.1 GHz × 2

3.3 ANN and GA Association

This section explains how the ANN and GA are combined to achieve the study goal. So, for a given number of hidden layers, the proposed algorithm begins with ten randomly generated individuals. Each individual is assessed. If the accuracy for any individual in the population is greater than or equal to a given maximum, the maximum is updated and saved. Simultaneously, each individual and its accuracy are saved. After evaluating these ten individuals, we take the best five from the backup and mutate and crossbreed them by returning a candidate population to the second generation. This process is repeated until the tenth generation, at which point the number of hidden layers is changed and the process restarted from the beginning. After evaluating the number of intervals in the hidden layers, four architectures emerge as the best, according to the algorithm. A diagram of such an association is shown in Fig. 5.

4. PROBLEM SOLUTION

This section presents the results obtained by applying the above-mentioned algorithms on the stator current signal modeled in Eq. (3). Table 1 gives the simulation parameters.

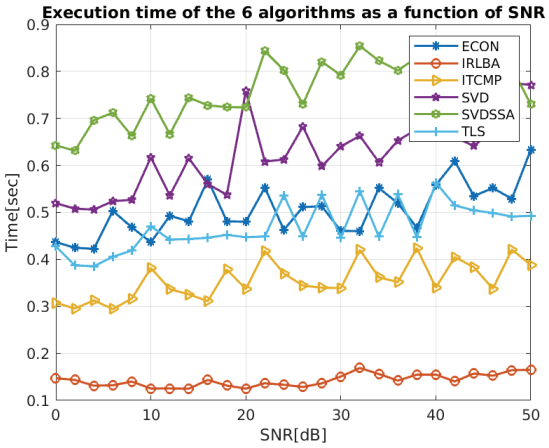

Fig. 6: Execution time of the six algorithms.

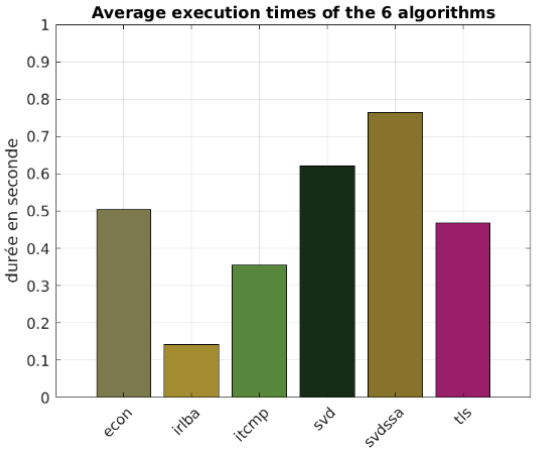

Fig. 7: Average execution time of the six algorithms.

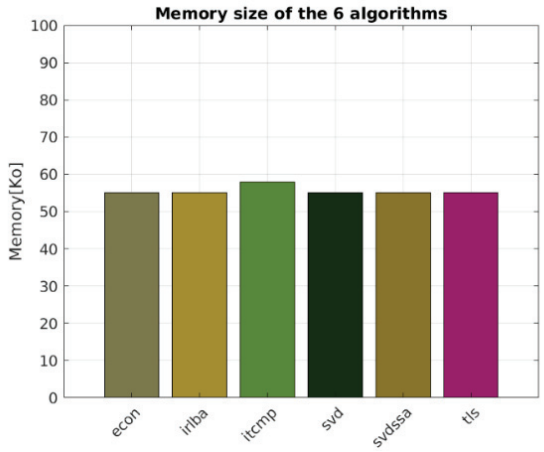

Fig. 8: Memory size of the six algorithms.

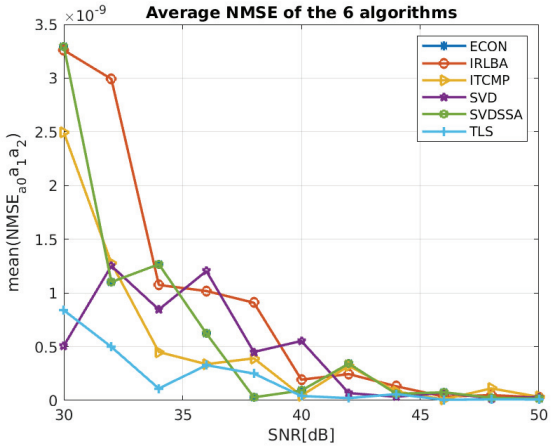

Fig. 9: Average NMSE on the amplitudes of the six algorithms.

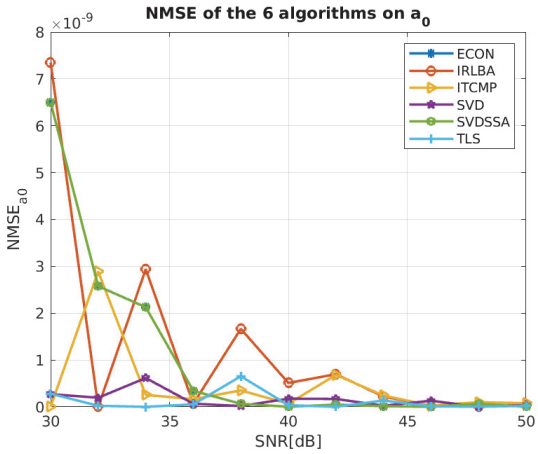

Fig. 10: NMSE on a_0 for the six algorithms.

4.1 Simulation Results for the ESPRIT Variants

In the first part of the simulation, identifying the best ESPRIT variant facilitates better discrimination of the bearing's fault characteristics. Accordingly, the performance of each variant is compared in terms of estimation, memory size, and execution time. In this simulation, only the frequencies characterizing a bearing fault are considered, namely: f_0 = 50 Hz, f_1 = 89.248 Hz, and f_2 = 189.248 Hz with the respective amplitudes: a_0 = 10 A, a_1 = 0.2 A, and a_2 = 0.07 A. The obtained results are shown in Fig. 6 which gives the time elapsed by each algorithm to detect the fault under SNR variation.

Figs. 7 and 8 illustrate the execution time and memory size occupied by the six algorithms to detect the harmonics and amplitudes characterizing a fault, based on the convergence curves. From the amplitude estimation in Figs. 9 and 10, it can be deduced that the ESPRIT-TLS variant is more efficient because it allows better parameter estimation. However, it is a little more expensive in terms of time than ESPRIT-IRLBA.

Moreover, the convergence of the studied algorithms for the fault amplitude estimation, depending on the variation in SNR values between 30 and 50 dB, is illustrated in Figs. 9 and 10.

***Table 2**: Results of the best architectures in the time domain according to the training data steps.*

Train step (dB)	Accuracy (%)	Other steps	Accuracy (%)	Time (s)	Memory (kB)
1	72.5	2	88.5	0.8011	148
		3	84.6	0.7971	148
		4	86.5	1.8338	188
2	88.46	1	72.54	3.6455	214
		3	84.61	1.7424	148
		4	86.53	1.6116	148
3	94.23	1	66.66	4.8352	214
		2	57.69	0.3613	148
		4	78.84	5.7682	148
4	82.69	1	73.52	5.5778	214
		2	73.07	0.3352	148
		3	82.69	0.3463	148

4.2 Results of ANN-GA Association

Once the variant that best estimates the amplitude and frequency parameters of a fault has been identified, all that remains is to prepare the training data in the form of two classes: healthy and defective. In addition, under the operating conditions of a rotating machine, the surrounding noise can vary and influence the stator current signal from one instant to another. In this study, it is modeled as a series of SNR step values taken in the interval $[1, 4]$ dB. Two datasets are used to prepare data for healthy and defective signals. The first contains the stator current signals represented in time, while the second contains a transformation of these signals in the frequency domain by application of the high-resolution ESPRIT-TLS method.

4.2.1 Preparation of the dataset

In the time domain, the dataset is only the signal of the stator current. It is used by extracting the amplitudes of the harmonics as inputs of the different ANN architectures modeled by GA to research the best architecture.

In the frequency domain, as well as amplitudes, the values of harmonics are added. This is why in the architecture in the frequency domain the input size increases to six.

4.2.2 Results

The results obtained respectively in the time and frequency domains are detailed in Tables 2 and 3. In this approach, for each learning step, whether in the time or frequency domain, a better neural architecture is sought using the genetic algorithm for the initial candidate parameters, i.e., the number of layers (varying between 1 and 4), the number of neurons in each layer (ranging from 1 to 10), and the activation functions in the layers (`logsig`, `tansig`, `hardlim` function) for the hidden layers and (`softmax`, `tansig`) for the output layer. The

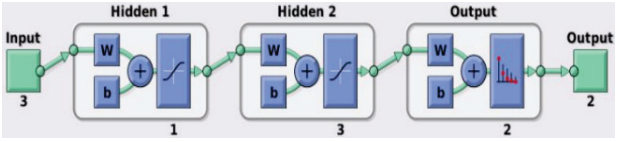

***Fig. 11**: Best architecture in the time domain.*

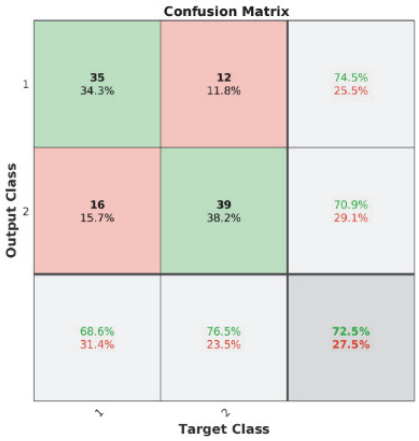

***Fig. 12**: Training with steps of 1 dB.*

application of the genetic algorithm for the optimization and training of the ANN by the stator current signal dataset yielded single hidden layer architectures using the `tansig` and the `softmax` functions in the output layer with the two neurons in the frequency domain and two hidden layers in the time domain having the same functions in both the hidden and output layers. The architectures obtained are tested on the prepared data formed according to the variation of the SNR ratio with increasing steps. This is to generalize the different architectures in the event of a sudden change in the SNR ratio. The training function used for the ANN is `trainbr` from MATLAB toolbox, with `mse` (mean squared normalized error) used as the performance function.

4.2.3 In the temporal domain

For the four learning steps (1, 2, 3, and 4), the respective numbers of neurons in the two hidden layers are: (5, 6), (1, 3), (1, 10), and (2, 7).

Table 2 presents all the best architecture in the time domain for each data step and their generalization on the other steps.

Finally, in the temporal domain, the best model retained is an architecture with two hidden layers, the first of which has a single neuron and the second three neurons. The activation functions are respectively `tansig` and `tansig`. As for the output layer with two neurons, the activation function retained by the genetic algorithm is `softmax`. This final architecture is presented in Fig. 11.

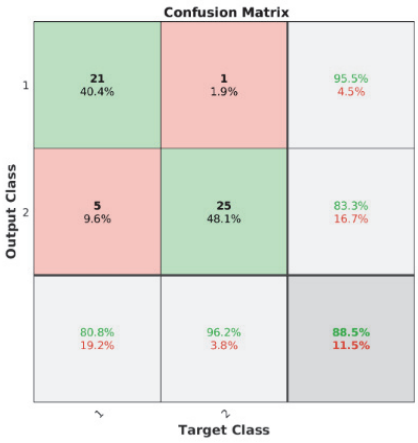

Fig. 13: Test on data with steps of 2 dB.

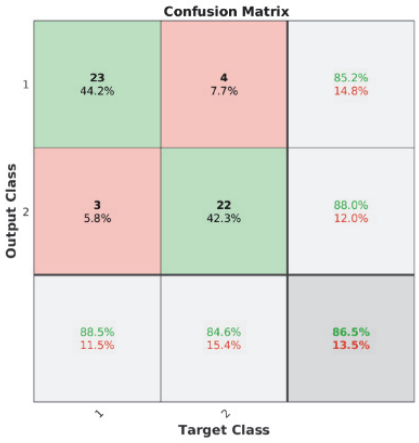

Fig. 15: Test on data with steps of 4 dB.

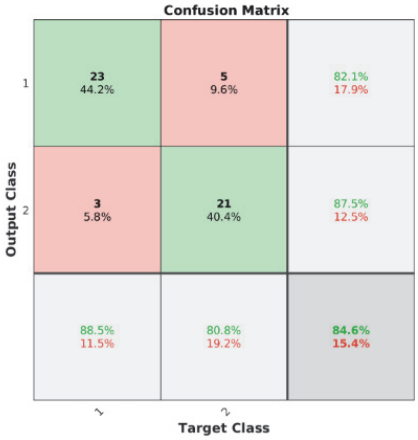

Fig. 14: Test on data with steps of 3 dB.

The confusion matrices for the 1 dB training step data as well as the other steps to assess its generalist are shown in Fig. 12. This confusion matrix translates the results of the best architecture on the training dataset. In this dataset, 51 represent the fault (machine with bearing fault) and the healthy machine (machine without bearing fault). Therefore, of the 102 datasets, in reality, 35 are healthy and 12 faulty but the matrix classifies them as healthy while 39 are really faulty and 16 wrongly healthy. So, the number in the green square represents the correct classification of that class and the number in the red square represents the wrong classification of that class and explains the percentages.

After this training step, the architecture is fed with the other data steps to see its generalization on them (how it classifies them). The other steps are 2, 3, and 4 dB, and the number of datasets 52 (26 healthy and 26 faulty).

Applying the same analogy with steps of 2 dB, on these 52 datasets, the last architecture above classified correctly 21 healthy and wrongly one healthy, 25 correctly faulty, and five wrongly faulty as shown in Fig. 13.

Applying the same analogy with steps of 3 dB, on these 52 datasets, the last architecture above classified correctly 23 healthy, wrongly five healthy, 21 correctly faulty, and three wrongly faulty as shown in Fig. 14.

Applying the same analogy here with steps of 4 dB, on these 52 datasets, the last architecture above classified correctly 23 healthy and wrongly four healthy, 22 correctly faulty, and three wrongly faulty as shown in Fig. 15.

4.2.4 In the frequency domain

For the four learning steps (1, 2, 3, and 4), the respective numbers of neurons in the two hidden layers are (4), (7), (9), and (7).

Table 3 also presents the best architecture in the frequency domain for each data step and their generalization on other steps.

Finally, in the frequency domain, the best model retained is an architecture with one hidden layer containing seven neurons. The activation function is `tansig`. As for the output layer with two neurons, the activation function retained by the genetic algorithm is `softmax`. Fig. 16 presents this final architecture.

The confusion matrixes on the 1 dB training step data and the other steps measure their generalists are shown in Fig. 17.

This confusion matrix translates the results of the best architecture on the training dataset. In this data, 52 datasets represent the fault (machine with bearing fault), and 50 the healthy machine (machine without bearing fault). Accordingly, for the 102 datasets, 50 are really healthy and zero faulty but it classifies them as healthy. Whereas 51 are really faulty and one which is wrongly healthy. So, the number in the green square represents the correct classification of that class and the number in the red square represents the wrong classification of that class and this explains these percentages.

After this training step, this architecture is fed with

***Table 3**: Results of the best architectures in the frequency domain according to the training data steps.*

Train step (dB)	Accuracy (%)	Other steps	Accuracy (%)	Time (s)	Memory (kB)
1	99	2	100	0.4125	115
		3	100	0.3195	115
		4	100	0.3135	115
2	100	1	99.01	0.5504	132
		3	100	0.2957	115
		4	100	0.3150	115
3	100	1	98.03	0.5097	132
		2	98.07	0.3239	115
		4	100	0.2254	115
4	100	1	98.03	0.5686	132
		2	98.07	0.3525	115
		3	98.07	0.3889	115

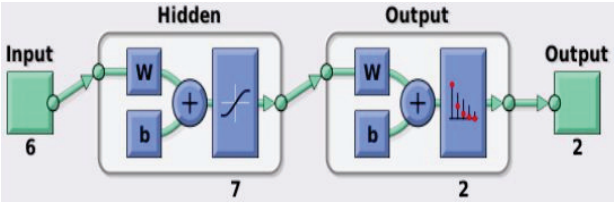

***Fig. 16**: Best architecture in the frequency domain.*

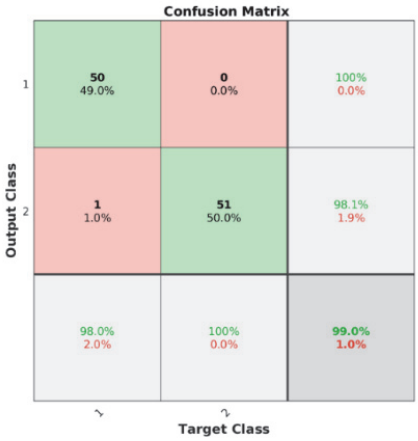

***Fig. 17**: Training with steps of 1 dB.*

other data steps to see its generalization on them (how it classifies them). The other steps are 2, 3, and 4 dB and the number in the dataset is 52 (26 healthy and 26 faulty).

Applying the same analogy to these 52 datasets with steps of 2 dB, the last architecture above classified correctly 26 healthy, wrongly zero healthy, 26 correctly faulty, and zero wrongly faulty as shown in Fig. 18.

Applying the same on these 52 datasets with steps of 3 dB, the last architecture above classified correctly 26 healthy, y zero wrongly healthy, 26 correctly faulty, and zero wrongly faulty as shown in Fig. 19.

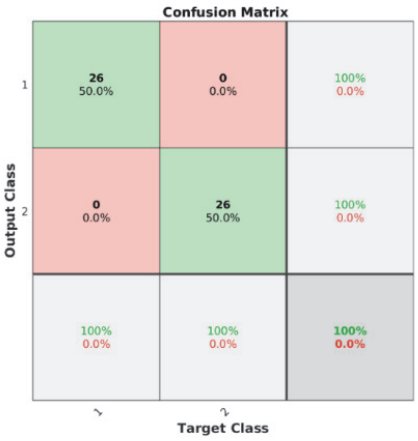

***Fig. 18**: Test on data with steps of 2 dB.*

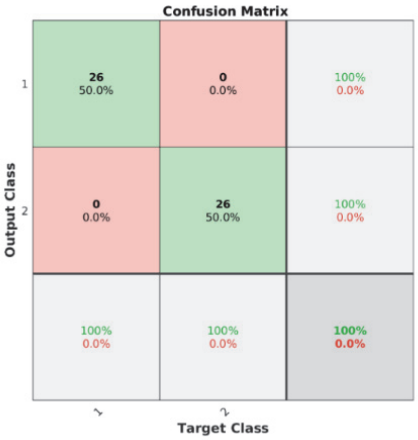

***Fig. 19**: Test on data with steps of 3 dB.*

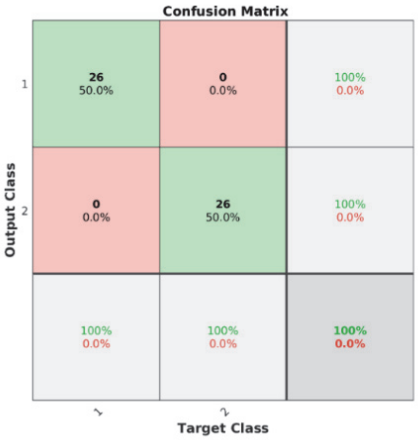

***Fig. 20**: Test on data with steps of 4 dB.*

Applying the same analogy to these 52 datasets with steps of 4 dB, the last architecture above classified correctly 26 healthy, wrongly zero healthy, 26 correctly faulty, and zero wrongly faulty as shown in Fig. 20.

4.3 Discussion

Compared to the time domain (Table 2) in terms of classification precision, elapsed time, and memory occupied to train the neural network, the frequency domain can be observed to give the best architectures to detect the bearing fault. This is because there is more information to describe the bearing fault in the frequency domain.

In addition, by comparing Fig. 7 and Table 3, it can be observed that the proposed approach which combines an ANN network driven by frequency signals obtained by applying the ESPRIT-TLS algorithm is strongly favored for early detection of a bearing fault in real time in comparison to the application of the ESPRIT-TLS algorithm alone. This applies not only to the execution time, but also the classification when considering ESPRIT-TLS alone since each parameter needs to be observed one by one to decide whether or not there is a fault. Therefore, with this combination all can be achieved simultaneously with low execution time.

Suffice to say, this combination is more efficient than ESPRIT-TLS alone.

5. CONCLUSION

The aim of this study was to seek, in the time or frequency domains, an ANN architecture or model which allows the real-time monitoring of each bearing defect. Based on two signal datasets, classified as healthy or faulty, the ANN was built and trained, and its performance then examined. The simulation results demonstrate that an ANN architecture can be developed which fulfills the need for precise satisfactory classification offering early detection in real time. Given their wealth of information, the stator current signals forming the used dataset in the frequency domain are better suited and favored for the training and design of such neural networks and the combination chosen can be a great help in monitoring the bearing fault in induction machines. In the future, it is recommended that this study be extended by applying the CNN (convolutional neural network), RNN (recurrent neural network), and machine learning methods to fault classification as well as determining the indicators of their expected robustness. In addition, experimental implementation of these algorithms is proposed on electronic board prototypes with a test bench to validate the simulation results.

REFERENCES

[1] S. Chakkor, M. Baghouri, and Abderrahmane Hajraoui, "High accuracy ESPRIT-TLS technique for wind turbine fault discrimination," *International Journal of Electrical and Computer Engineering*, vol. 9, no. 1, pp. 122–131, 2015.

[2] B. D. Ketelaere, M. Hubert, and E. Schmitt, "Overview of PCA-based statistical process-monitoring methods for time-dependent, high-dimensional data," *Journal of Quality Technology*, vol. 47, no. 4, pp. 318–335, 2015.

[3] Z. Husain, H. Malik, and M. A. Khan, "Recent trends in power transformer fault diagnosis and condition assessment," *Buletin Teknik Elektro dan Informatika*, vol. 2, no. 2, pp. 95–104, Jun. 2013.

[4] D. Wu *et al.*, "An automatic bearing fault diagnosis method based on characteristics frequency ratio," *Sensors*, vol. 20, no. 5, 2020, Art. no. 1519.

[5] C. Abdelkrim, M. S. Meridjet, N. Boutasseta, and L. Boulanouar, "Detection and classification of bearing faults in industrial geared motors using temporal features and adaptive neuro-fuzzy inference system," *Heliyon*, vol. 5, no. 8, Aug. 2019, Art. no. e02046.

[6] B. Zhang, C. Sconyers, C. Byington, R. Patrick, M. E. Orchard, and G. Vachtsevanos, "A probabilistic fault detection approach: Application to bearing fault detection," *IEEE Transactions on Industrial Electronics*, vol. 58, no. 5, pp. 2011–2018, May 2011.

[7] J. Zarei, M. A. Tajeddini, and H. R. Karimi, "Vibration analysis for bearing fault detection and classification using an intelligent filter," *Mechatronics*, vol. 24, no. 2, pp. 151–157, Mar. 2014.

[8] P. Gupta and M. Pradhan, "Fault detection analysis in rolling element bearing: A review," *Materials Today: Proceedings*, vol. 4, no. 2, pp. 2085–2094, 2017.

[9] H.-Q. Wang, W. Hou, G. Tang, H.-F. Yuan, Q.-L. Zhao, and X. Cao, "Fault detection enhancement in rolling element bearings via peak-based multiscale decomposition and envelope demodulation," *Mathematical Problems in Engineering*, vol. 2014, 2014, Art. no. 329458.

[10] S. A. Chopade, J. A. Gaikwad, and J. V. Kulkarni, "Bearing fault detection using PCA and wavelet based envelope analysis," in *2nd International Conference on Applied and Theoretical Computing and Communication Technology (iCATccT)*, Bangalore, India, 2016, pp. 248–253.

[11] T. H. Mohamad and C. Nataraj, "Fault identification and severity analysis of rolling element bearings using phase space topology," *Journal of Vibration and Control*, vol. 27, no. 3–4, pp. 295–310, 2021.

[12] M. L. Masmoudi, E. Etien, S. Moreau, and A. Sakout, "Single point bearing fault diagnosis using simplified frequency model," *Electrical Engineering*, vol. 99, pp. 455–465, Mar. 2017.

[13] D. D. Susilo, A. Widodo, T. Prahasto, and M. Nizam, "Fault diagnosis of roller bearing using parameter evaluation technique and multi-class support vector machine," *AIP Conference Proceedings*, vol. 1788, no. 1, 2017, Art. no. 030081.

[14] Y. Imaouchen, R. Alkama, and M. Thomas, "Bearing fault detection using motor current signal analysis based on wavelet packet decomposition and Hilbert envelope," *MATEC Web of Conferences*, vol. 20, 2015, Art. no. 03002.

[15] S. Zhang, S. Zhang, B. Wang, and T. G. Habetler, "Deep learning algorithms for bearing fault diagnostics - a review," in *IEEE 12th International Symposium on Diagnostics for Electrical Machines, Power Electronics and Drives (SDEMPED)*, Toulouse, France, 2019, pp. 257–263.

[16] B. Aubert, "Détection des courts-circuits interspires dans les Générateurs Synchrones à Aimants Permanents : Méthodes basées modèles et filtre de Kalman étendu - Application à un canal de génération électrique en aéronautique," Ph.D. dissertation, Institut National Polytechnique de Toulouse - INPT, Toulouse, France, 2014.

[17] J. Chatelain, *Machines électriques*. Lausanne, Switzerland: Ecole Polytechnique Fédérale de Lausanne, 1983.

[18] S. A. S. A. Kazzaz and G. Singh, "Experimental investigations on induction machine condition monitoring and fault diagnosis using digital signal processing techniques," *Electric Power Systems Research*, vol. 65, no. 3, pp. 197–221, Jun. 2003.

[19] W. T. Thomson and R. J. Gilmore, "Motor current signature analysis to detect faults in induction motor drives—fundamentals, data interpretation, and industrial case histories," in *Proceeding of the Thirty-Second Turbomachinery Symposium*, 2003, pp. 145–156.

[20] A. Gheitasi, "Motors fault recognition using distributed current signature analysis," Ph.D. dissertation, Auckland University of Technology, New Zealand, 2013.

[21] W. T. Thomson, "On-line motor current signature analysis prevents premature failure of large induction motor drives," *Maintenance and Asset Management*, vol. 24, no. 3, pp. 30–35, May 2009.

[22] S. Chakkor, "E-diagnostic de processus physiques à base des méthodes de haute résolution Application : machines éoliennes," Ph.D. dissertation, Université Abdelmalek Essaâdi, Tangier, Morocco, 2015.

[23] K. Kudelina *et al.*, "Bearing fault analysis of BLDC motor for electric scooter application," *Designs*, vol. 4, no. 4, 2020, Art. no. 42.

[24] M. Unal, M. Onat, M. Demetgul, and H. Kucuk, "Fault diagnosis of rolling bearings using a genetic algorithm optimized neural network," *Measurement*, vol. 58, pp. 187–196, Dec. 2014.

[25] L. Jack and A. Nandi, "Genetic algorithms for feature selection in machine condition monitoring with vibration signals," *IEE Proceedings - Vision, Image, and Signal Processing*, vol. 147, no. 3, pp. 205–212, Jun. 2000.

Pascal Dore received his bachelor's degree in Mathematical and Computer Sciences and master's degree in Communication and Embedded Electronic Systems. He is currently a Ph.D. student at the National School of Applied Sciences of Tangier, Morocco, in the Information and Communication Techniques Laboratory and works on the detection of electromechanical faults in inductive machines by spectral analysis by application of high-resolution signal processing algorithms and artificial intelligence algorithms.

Saad Chakkor received his master's degree in Electrical and Computer Engineering from the Faculty of Sciences and Techniques of Tangier, Morocco in 2002. He continued his studies to obtain the ENS of Rabat diploma in the computer science specialty in 2003. In 2006, he received DESA diploma in Automatics and information processing at the FST of Tangier, Morocco. Thereafter, He obtained the doctorate degree in Automatics and Telecommunications from the Faculty of Sciences of Tetouan, Morocco in 2015. He has taught at several educational institutions. Currently, he works teacher of Telecommunications in the ENSAT School. He is a member in the Information and Communication Technology Laboratory (LabTIC), National School of Applied Sciences in Tangier, University of Abdelmalek Essaâdi, Morocco. His research areas are telecommunications systems, mobile networks, cognitive radio, wireless intelligent sensors networks and theirs applications, frequency estimation algorithms, automation, detection and diagnosis systems using signal processing methods.

Mostafa Baghouri received his DESA degree in Automatic and Information Processing at the FST of Tangier, Morocco in 2006, and Ph.D. degree in Physics Specialty Embedded Systems from the Faculty of Science, Tetouan Abdelmalek Essaadi University, Morocco in 2016. He is a researcher in Wireless Sensor Networks since 2006.

Ahmed El Oualkadi received his Ph.D. degree in electrical engineering from the University of Poitiers, France, in 2004. From 2000 to 2003, he was a research assistant at the Electronics & Electrostatics Research Unit at the University of Poitiers, France. In 2004, he was an assistant professor at University Institute of Technology, Angoulême, France. During this period, he worked, in collaboration with EADS-TELECOM, on various European projects which concern the nonlinear analysis & RF circuit design of switched- capacitor filters for radio-communication systems. Currently, he is a professor at the department of information and communication systems at the National school of applied sciences of Tangier, Abdelmalek Essaadi University, Morocco, where he is the coordinator of both the Graduate engineering program in Telecommunication Systems and Networks and the Master program in Communication Systems and Embedded Electronics. His research interests include analog IC, mixed-signal and RFIC design for wireless communication, embedded system applications and wireless communications. He has supervised several PhD and Masters Theses and has been the principal investigator and the project manager for several international and bilateral research projects.